

Power Generation for a 2D Tethered Wing Model with a Variable Tether Length

Ashwin Ramesh, Mario W. Gomes

Rochester Institute of Technology
76 Lomb Memorial Drive, Rochester, NY 14623, USA
acr2810@rit.edu; mwgeme@rit.edu

Abstract - Conventional wind turbines are a mature technology. Incremental improvements can be made, but order of magnitude increases in performance are unlikely. However, tethered wings are a potentially transformative approach to harvesting wind energy and have the potential for large performance increases. However, the optimum design for these tethered wing systems is still an open question. We examine a simplified, pumping, tethered wing system for generating power. To explore the effect of tether pumping on power generation, we created a numerical simulation of a 2D system. In our simulation each half cycle consists of two phases: a pull-in phase in which we spend a small amount of power to bring the air frame up to speed and a reel-out phase in which we extract power from the system as the tether is unwound from a drum. Since the power consumed and obtained is calculated as a function of tension force across the tether, conclusions for variation in power during both phases is examined with respect to the tension force. Using this 2D simulation, we find that an average cycle power of 5.2 W can be generated at the end of the reel-out phase.

Keywords: high altitude energy, tethered airfoil, wind turbine, renewable energy.

1. Introduction

The use of tethered structures to harness wind energy goes back to the 18th century. Pocock (1851) discusses how large kites were able to pull a carriage with passengers by harnessing wind energy. Power generated by a wind turbine is a function of wind speed and density of the medium going over the blades. The wind power available per unit area of swept blades can be written as shown in Eqn. 1.

$$\delta = 0.5\rho V_w^3 \quad (1)$$

Archer *et al.* (2009) determined that for some regions of the earth above 2,000 m the wind power density increases with height and the altitude range between 500 m and 2,000 m has relatively constant wind power densities. They also determined that the highest wind power densities are available at altitudes between 8,000 m and 10,000 m. Modern day turbines have a maximum nacelle heights of approximately 120 m. Tethered systems can be designed to harvest these promising high altitude winds. Loyd (1980) analysed the power production capabilities of several simple tethered, or kite, systems. This paper explores and expands upon the crosswind motion model discussed by Loyd to harvest wind energy. Goela *et al.* (1986) created and examined a simplified model of a water pumping system using a kite. Goela *et al.*'s kite pumping system consists of three main parts : an aerodynamic body, an energy conversion system, and a tether that connects the aerodynamic body to the energy conversion system. They found that this simple model was capable of producing positive power to a cyclic water pump. Some researchers have conducted experiments to control the motion of actual power generating kites. For example, Lansdorp *et al.* (2007) examined how a kite's path can be controlled by varying the orientation of a surfkite by mounting servos on the kite itself.

The model we examine here is a 2D hydrokite model. McConnaghy (2012) analysed power generation of a hydrokite system. This system is essentially an underwater kite which exploits cross-flow motion to harness hydropower. Hydrokite systems could be used to transform kinetic energy in a river

into useable electrical energy. Similar to Goela’s simple kite model which consisted of an ascent stroke and a descent stroke, McConnaghy’s model consisted of a deploy and a return stroke. The model we examine here is an extension of the McConnaghy’s 2D steady-state model that consisted of a rigid boom, a hydrofoil and a fixed beta for each stroke. In our study we look at how changing the tether length and the orientation of the wing/airframe can affect its path and the system’s power production.

2. System Description

Our system consists of an aerodynamic body (wing), a tether, and a base station. The tether connecting the aerodynamic body is wrapped around a drum, at the base station located on the ground, which in turn is connected to an electric generator. The aerodynamic forces acting on the wing produce a tension force on the tether. When the tether is unwound from the drum due to the aerodynamic forces acting on the wing, power is generated at the base station. High lift forces can be achieved by varying the angle of attack of the airfoil, which can be controlled by changing β , as seen in Fig. 1. We split one complete cycle of our system into two halves, the deploy and return strokes. We analyse the first half of the cycle, since the second half of the cycle is very similar to the first.

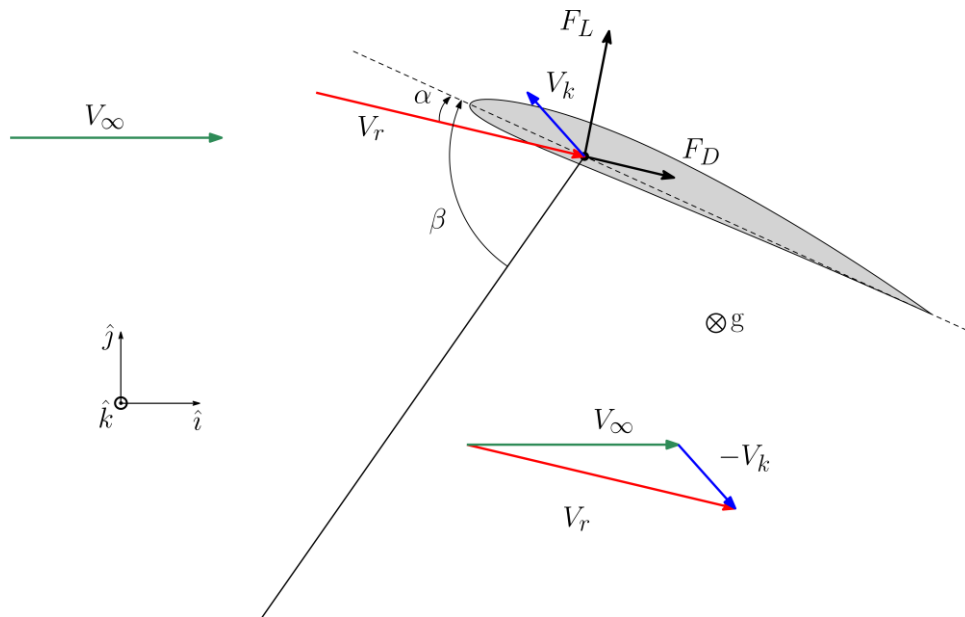


Fig. 1. A top-view schematic of our hydrokite system showing velocities and aerodynamic forces acting on the system.

Each half cycle of this system consists of two phases. Since we start the cycle with the kite stationary, and we need to quickly accelerate the kite to maximize energy production in the cross-wind motion. Energy is spent on the system during the pull-in phase of the half cycle. A desired fixed wing angle (β) is chosen and the tether connecting the airframe is reeled in. This increases the relative velocity of the wing. The reel-in phase of the half cycle ends once the desired angular velocity of the tether is reached. Power is then generated at the ground station during the next reel-out phase of the half cycle. At the beginning of the second phase, a new wing angle (β) is chosen and the tether is reeled out until the tether reaches zero angular velocity.

In an effort to simplify a complex system to improve understanding, we chose to model the cross-wind motion of our system in two dimensions. To obtain optimum power output from the system, the power generated should be maximized during the second phase and the power consumed should be minimized during the first phase. The main aim of this study is to determine the conditions which maximize the average power output for one half-cycle. The equations of motion are discussed in the second section along with the assumptions made to model this system. The performance of the kite

depends on the parameters such as tension loads and the aerodynamic forces the kite system experiences, which in turn are a function of the relative wind velocity. Performance also depends on parameters such as the hydrokite angle, initial angular velocity of the tether, tether length velocity, wing span, kite mass, and initial tether angle. The forces acting on the airfoil are shown in Fig. 1. Steady-state lift and drag coefficients from Sheldahl *et al.* (1981) are used to determine the aerodynamic forces. The relative velocity of the wind, \vec{V}_{rel} , is calculated using Eqn. 2, where \vec{V}_{∞} is the free stream velocity and \vec{V}_k is the velocity of the kite, and F_L and F_D are the lift and the drag forces acting on the system respectively.

$$\vec{V}_{rel} = \vec{V}_{\infty} - \vec{V}_k \quad (2)$$

Both the reel-in and the reel-out phases are depicted in Fig.2. The angle, β_1 , shown in the figure represents the fixed hydrokite angle during the reel-in phase and β_2 represents the hydrokite angle during the reel-out phase. The constant pull-in and the reel-out rates are represented by the \dot{L}_1 and \dot{L}_2 respectively as shown in Fig.2.

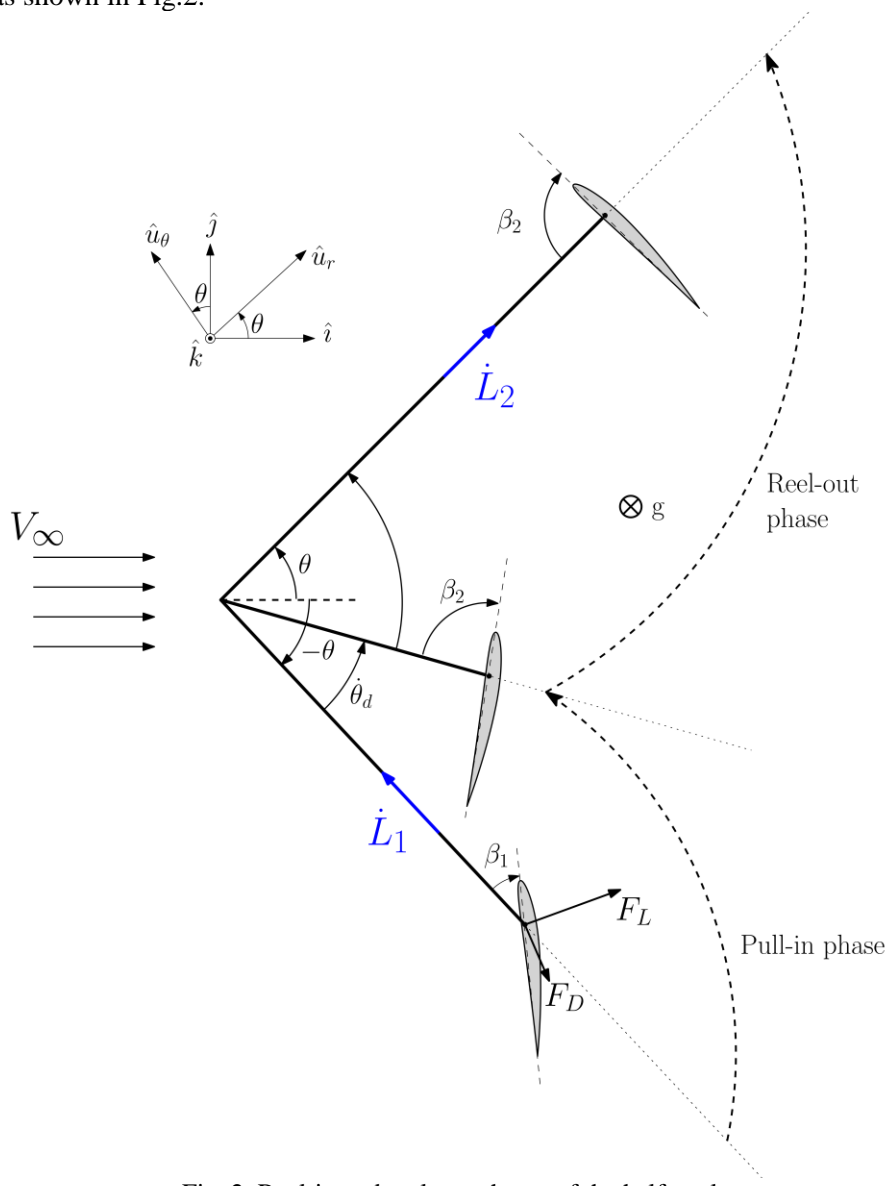


Fig. 2. Reel-in and reel-out phases of the half-cycle.

Our model of this system assumes the following: the tether is massless, rigid and a straight line, tether drag is neglected and does not affect the power generated by the system, fixed beta values are used for both phases of the half cycle, the wing is mounted at the quarter-chord point and thus we neglect any aerodynamic moment about the contact point, that the wing can flip orientation (β) instantly with no energetic cost, and that all motion occurs on the horizontal plane.

3. Simulation and Equations of Motion

This system's non-linear equations of motions were determined and the system was simulated in MATLAB. Numerical solutions to the equations of motion were determined using MATLAB's ODE45 variable-step size, 4th order, Runge-Kutta integration routine. The position of the kite is as shown in Eqn. 3, where l is the tether length and \hat{u}_r is the unit vector as shown in the Fig 2. The tether tension would be in the negative \hat{u}_r direction as represented in the Eqn. 4. The instantaneous power is calculated using Eqn. 5, where P is the instantaneous power.

$$\vec{r} = l\hat{u}_r \quad (3)$$

$$\vec{T} = -T\hat{u}_r \quad (4)$$

$$P = \vec{T} \cdot \dot{l}\hat{u}_r \quad (5)$$

The velocity of the kite is obtained by taking a derivative of the position vector as shown in Eqn. 6.

$$\vec{V}_k = \dot{\vec{r}} = \dot{l}\hat{u}_r - l\dot{\theta}\hat{u}_\theta \quad (6)$$

The lift and drag force magnitudes are calculated as shown in the Eqn.s 7 and 8 respectively.

$$L = 0.5\rho AV_{rel}^2 C_L \quad (7)$$

$$D = 0.5\rho AV_{rel}^2 C_D \quad (8)$$

C_L and C_D are the three dimensional lift and drag coefficients. Although the system is modeled in two dimensions, the lift and drag forces are calculated in three dimensions to account for a finite span wing. The 3D lift and drag coefficients are obtained from the 2D coefficients by using standard induced drag and induced angle of attack corrections as shown in Eqn. 9 where AR is the aspect ratio, and c_l and c_d are the 2D lift and drag coefficients. The airfoil profile chosen for the study here is a NACA 0015.

$$C_D = c_d + \frac{c_l^2}{\pi e AR} \quad (9)$$

The Span Efficiency Factor represented by e as shown in the Eqn. 9 corresponds to how elliptical the planform of the wing is. For a perfectly elliptical wing e would be one, we assume $e=0.9$. The c_l and c_d are obtained by determining the angle of attack α , and then interpolating the α to get accurate values of c_l and c_d from the table look up of experimental 2D data. This experimental data was obtained from a study which measured 2D lift, drag and moment coefficients for symmetric airfoils. Sheldahl *et al.* (1981).

$$\ddot{\vec{r}} = \ddot{l}\hat{u}_r + \dot{l}\dot{\theta}\hat{u}_\theta + l\ddot{\theta}\hat{u}_\theta - l\dot{\theta}^2\hat{u}_r \quad (10)$$

$$\vec{T} + \vec{L} + \vec{D} = m\ddot{\vec{r}} \quad (11)$$

The tension, lift, and drag forces appear in the linear momentum balance equation shown in Eqn. 11. The resulting equation of motion for $\vec{\theta}$ is then numerically determined from Eqn. 11. Once an approximate solution is obtained using numerical integration, the average cycle power is calculated using Eqns. 12 and 13, where t_f is the final cycle time.

$$E_{cycle} = \int_{t_i}^{t_f} P dt \quad (12)$$

$$P_{avg} = \frac{E_{cycle}}{t_f - t_i} \quad (13)$$

3. Results and Discussion

The performance of this system is evaluated based on the average power produced in the half cycle. With a given set of initial parameter values as shown in Table 1, the study for the optimum β for both the phases of the cycle was conducted. The study was conducted for various beta values varying between $0^\circ - 180^\circ$ and different reel-in rates. The tether was reeled in at a constant rate till a desired tether angular velocity of 1.5 rad/sec was reached. Fig. 3 shows the time taken to reach a desired angular velocity changes for change in β and \dot{l} . At the beginning of the reel-in phase a fixed β is chosen such that the time taken to reach the desired angular velocity is small.

Table 1. Parameter values used in the simulation.

Parameter	Symbol	Values
Airframe mass	m	1kg
Initial tether length	l	5 m
Span of aerofoil	b	1 m
Chord length	c	1/6 m
Free stream velocity	V_∞	5 m/s
Initial angle of tether	θ	-70 [deg]

Fig. 4 shows the average power for each half cycle for various beta values. The hydrofoil angle for which the average power is a minimum is not necessarily the β which uses the least energy as there is a possibility that although the average power might be minimal, the time which it took to reach the desired angular velocity might be large. The optimum hydrofoil angle is chosen such that the energy used to reach a desired angular velocity is minimum and the time it takes to reach the given angular velocity is minimum. The optimum β is chosen by comparing the results between the Fig. 3 and Fig. 4. From Fig. 3 it is seen that as the reel-in rate changes the optimum beta values also change. From the simulation it is observed that for reel-in rates tested we see that fortunately, smaller beta values take up lesser time to reach the desired angular velocity and also require less energy.

Once the reel-in phase is completed, the reel-out phase is initiated. In the reel-out phase the tether is let out till zero angular velocity is reached and the power is generated as the tether is unwound at the ground station. For the system to shift from the reel-in phase to the reel-out phase the airframe must change its orientation. Here a new optimum beta value is chosen for the reel-out phase. In our simulation it is assumed that this change in orientation of the airframe does not consume any time or power. This assumption is made on the basis that the time and the power required will likely be small relative to the power generated over the whole cycle.

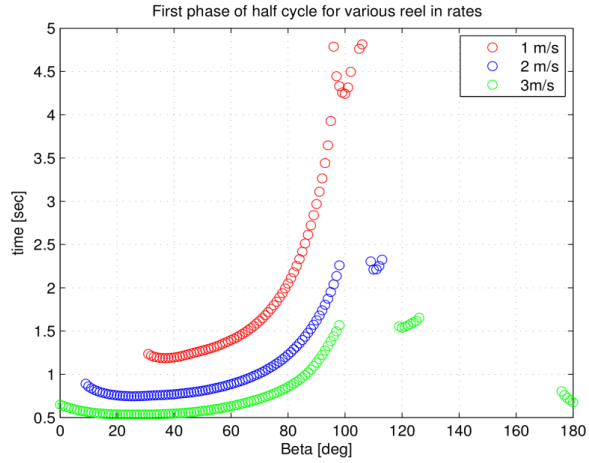


Fig. 3. Time taken to reach a desired angular velocity for various beta values.

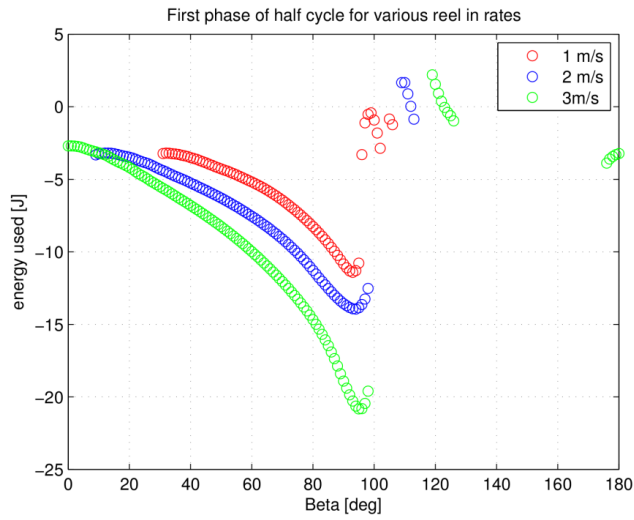


Fig. 4. Energy consumed as a function of hydrofoil angle for the reel-in phase.

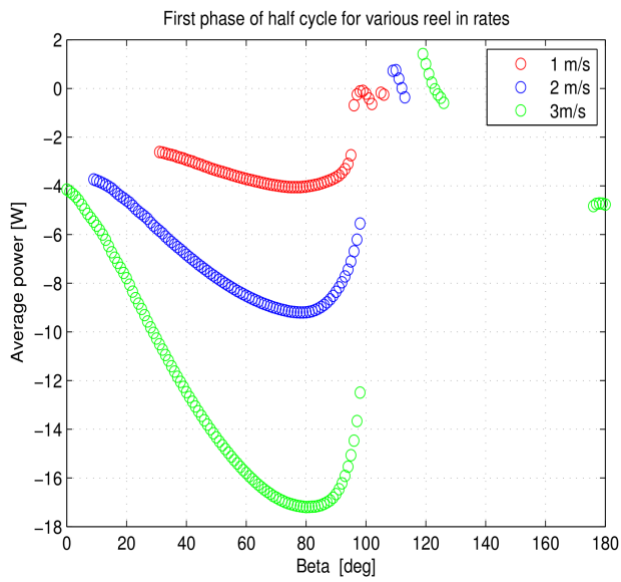


Fig. 5. Average power as a function of hydrofoil angle.

The Figs. 6 and 7 show the change in instantaneous power and tension with time. During the reel-out phase, the rate of change of tether length is constant as a result it can be seen that as the tension loads decreases, the power generated is proportional to that in the reel-out phase. Although the results obtained here are for a half-cycle, the second half of the cycle will likely be similar to the first half.



Fig. 6. Instantaneous power decreases with time in the reel-out phase.

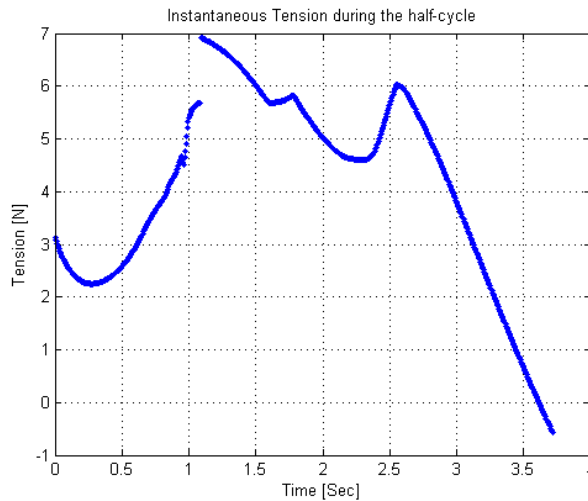


Fig. 7. Tension force is proportional to the instantaneous power during the reel-out phase.

4. Conclusion

To achieve a positive power production, the power produced during the reel-out phase must be more than the power consumed during the reel-in phase. The results show that an average half cycle power of 5.29 W can be obtained. Although the average power developed per half cycle ranges between 5-10 W depending on the system parameters. Power production is affected by system parameters such as wing size and wing speed. Although the simulation is only examined for the half-cycle, it can be predicted that the second half of the cycle is likely to be the same. This assumption is made since the tether and the wing come to a zero velocity state at the end of each cycle. From our study we also learn that allowing the beta angle to change during the reel-in and the reel-out phases improves the performance of the system.

However we predict that improvements can be made in the tether and beta control to also increase the performance.

References

- Archer C., Calderia K. (2009). "Global Assessment of High-Altitude Wind Power". *Energies* ,2, 307-319.
- Goela J., Vijaykumar R., and Zimmermann R. (1986). "Performance Characteristics of a Kite Powered Pump". *Journal of Energy Resources Technology*,108, pp. 188-193.
- Lansdorp B., Ruitkamp R., and Ockels W. (2007). "Towards flight testing of remotely controlled surfkites for wind energy generation". AIAA Paper.
- Loyd M.(1980). "Crosswind Kite Power". *Journal of Energy*, 4, 3, pp.106-111.
- McConnaghy K. (2012). "Analysis of Translating Hydrofoil Power Generation Systems (Hydrokites)". MS Thesis.
- Patrick J Moriarty, A Craig Hansen(2005) . *AeroDyn Theory Manual*. Technical Report December.
- Pocock G.(1851). "A treatise on the aeropleustic art". Longman, Brown and Co.
- Sheldahl R., Kilmes P. (1981). "Aerodynamic Characteristics of Seven Symmetrical Airfoil Sections Through 180-Degree Angle of Attack for Use in Aerodynamic Analysis of Vertical Axis Wind Turbines". Technical report, Sandia National Laboratories.